

## An efficient modulation scheme for dual beam polarimetry

K. Nagaraju\*, K. B. Ramesh, K. Sankarasubramanian<sup>†</sup> and  
K. E. Rangarajan

*Indian Institute Astrophysics, Bangalore 560 034, India*

*<sup>†</sup>ISRO Satellite center, Bangalore 560 094, India*

Received 16 April 2007; accepted 27 July 2007

**Abstract.** An eight stage balanced modulation scheme for dual beam polarimetry is presented in this paper. The four Stokes parameters are weighted equally in all the eight stages of modulation resulting in total polarimetric efficiency of unity. The gain table error inherent in dual beam system is reduced by using the well known beam swapping technique. The wavelength dependent polarimetric efficiencies of Stokes parameters due to the chromatic nature of the waveplates are presented. The proposed modulation scheme produces better Stokes  $Q$  and  $V$  efficiencies for wavelengths larger than the design wavelength whereas Stokes  $U$  has better efficiency in the shorter wavelength region. Calibration of the polarimeter installed as a backend instrument of the Kodaikanal Tower Telescope is presented. It is found through computer simulation that a 14% sky transparency variation during calibration of the polarimeter can introduce  $\approx 1.8\%$  uncertainty in the determination of its response matrix.

*Keywords :* instrumentation : polarimeter — technique : polarimetric

### 1. Introduction

Polarimetric accuracy is one of the most important goals in modern astronomy. It is limited since most optical elements encountered by the light on its path from the source to the detector, can alter its state of polarization (for eg. telescope optics, imaging system, grating, etc). Apart from these, variation in sky transparency, image motion and

---

\*e-mail:nagaraj@iiap.res.in

blurring due to the atmosphere are a major concern in high precision ground based solar polarimetry. The effect of atmosphere, which is commonly known as seeing induced effect, can be reduced by fast modulation schemes (Stenflo & Povel 1985). The modulation frequencies in these schemes are generally higher than seeing fluctuations, which is  $\approx 1$  kHz (Stenflo & Povel 1985; Lites 1987). Large format CCDs, which are required to cover reasonable spectral and spatial range, will pose difficulty in reading out the data at kHz speed. Stenflo & Povel (1985) proposed a scheme whereby rapidly modulated signal is demodulated by optical means, thereby avoiding the need to read the detectors at a rapid rate. Lites (1987) has proposed a rotating waveplate modulation scheme as an alternative to minimize the seeing induced cross-talk among Stokes parameters. There it is shown that the faster the rotation rate of the modulator, the lower the cross-talk among Stokes parameters. And the seeing induced cross-talk levels of a dual beam system are factors 3-5 smaller than those of a single beam system. However, in dual beam system, the error introduced due to flat field residual is a matter of concern in high precision polarimetry. A possible solution to the above mentioned problems can be found by using a mixed scheme in which spatial and temporal modulations are performed (Elmore et al. 1992; Martinez Pillelt et al. 1999; Sankarasubramanian et al. 2003). The gain table uncertainties are avoided using the beam swapping technique (Donati et al. 1990, Semel et al. 1993; Bianda et al. 1998)

A low cost dual beam polarimeter has been installed as a backend instrument for the Kodaikanal Tower Telescope (KTT). Different modulation schemes were studied and an optimum scheme is identified. The proposed scheme requires eight stages of modulation of input light in order to obtain the maximum polarimetric efficiency. Laboratory experiments have been performed to verify the theoretical understanding of the proposed scheme. The studies are extended to other wavelengths apart from the design wavelength of  $\lambda 6300$ .

The outline of this paper is as follows. The proposed eight stage modulation scheme for the measurement of general state of polarization is discussed in section(2). Wavelength dependence of the efficiency of the polarimeter in measuring Stokes parameters is presented in section(3). In section(4), the performance of the polarimeter at KTT is presented.

## 2. Proposed modulation scheme

A zero-order quarter wave (R1) and a zero-order half wave (R2) retarders at  $\lambda 6300$  are chosen as the modulators for the proposed polarimeter. R1 and R2 are the first and second elements of the polarimeter, as seen by the incoming light, followed by a polarizing beam splitter cube (PBS). The PBS has an extinction ratio  $> 10^3$  with respect to a polarizing Glan-Thomson prism (GTP). A simplest way of measuring Stokes parameters is to use a half waveplate (HWP) along with PBS for linear polarization measurement and a quarter waveplate (QWP) along with PBS for circular polarization measurement (Bianda et al.

1998). However, this way of modulation will introduce a possible differential optical aberrations between the linear and circular polarization measurements due to different optical elements encountered by the light. Using both the waveplates during all stages of measurements or using a single retarder with an appropriate retardance can avoid the differential aberrations (Lites 1987; Elmore et al. 1992). The modulation scheme presented here uses both R1 and R2 in all stages of measurements.

## 2.1 Modulation

The input polarization is modulated on to intensity by using the waveplate orientations given in Table 1.

**Table 1.** Orientation of waveplates for different stages of modulation expressed in degrees.

Modulation stage	Orientation of QWP(R1)	Orientation of HWP(R2)
1	22.5	0
2	22.5	45
3	67.5	45
4	67.5	90
5	112.5	90
6	112.5	135
7	157.5	135
8	157.5	180

The modulated intensities  $\vec{I}^\pm = (I_1^\pm, I_2^\pm, I_3^\pm, I_4^\pm, I_5^\pm, I_6^\pm, I_7^\pm, I_8^\pm)^T$ , where  $T$  represents transpose operator, can be written in terms of input Stokes parameters as

$$\vec{I}^\pm = g^\pm \mathbf{O}^\pm \vec{S}_{in} \quad (1)$$

where  $\pm$  indicate the two orthogonally polarized beams emerging out of the polarimeter respectively.  $\vec{S}_{in} = [I, Q, U, V]^T$  is the input Stokes vector to the polarimeter. Here, the standard definition of the Stokes vector is used with  $I$  representing the total intensity,  $Q$  and  $U$  representing the linear polarization state and  $V$  representing the circular polarization state. The multiplication factor of the two orthogonally polarized beams  $g^\pm$ , known as the gain factor, is a product of transparency of the corresponding optical path and the detector gain factor. The analyser Mueller matrices of respective beams can be obtained by multiplying the Mueller matrices of retarders ( $\mathbf{M}_{R1}$  and  $\mathbf{M}_{R2}$ ) and PBS ( $\mathbf{M}_P^\pm$ ) in the order  $\mathbf{M}_P^\pm \mathbf{M}_{R2} \mathbf{M}_{R1}$  (del Toro Iniesta 2003; Stenflo 1994). The modulation matrices  $\mathbf{O}^\pm$  are constructed by arranging the first row of the analyser matrix of the respective beam for each of the measurement steps (see del Toro Iniesta 2003 for details).

The theoretical modulation matrices  $\mathbf{O}^\pm$  at the design wavelength are given below.

$$\mathbf{O}^\pm = 0.5 \begin{pmatrix} 1.0 & \pm 0.5 & \mp 0.5 & \pm 0.707 \\ 1.0 & \mp 0.5 & \pm 0.5 & \mp 0.707 \\ 1.0 & \mp 0.5 & \mp 0.5 & \mp 0.707 \\ 1.0 & \pm 0.5 & \pm 0.5 & \pm 0.707 \\ 1.0 & \pm 0.5 & \mp 0.5 & \mp 0.707 \\ 1.0 & \mp 0.5 & \pm 0.5 & \pm 0.707 \\ 1.0 & \mp 0.5 & \mp 0.5 & \pm 0.707 \\ 1.0 & \pm 0.5 & \pm 0.5 & \mp 0.707 \end{pmatrix}.$$

It is to be noted here that the four Stokes parameters are modulated on to intensity in all the eight stages of measurements. Also that in all the eight stages of measurements, each Stokes parameter is weighted equally. Matrices  $\mathbf{O}^\pm$  show that the alternate measurements are obtained by swapping the orthogonally polarized beams (seen as sign change in the corresponding Stokes parameters).

The maximum efficiencies of the modulation scheme (see del Toro Iniesta & Collados 2000; del Toro Iniesta 2003 for details) in measuring Stokes  $I$ ,  $Q$ ,  $U$ ,  $V$  are 1.0, 0.5, 0.5, 0.707 respectively, at the design wavelength. The total polarimetric efficiency is  $\sqrt{0.5^2 + 0.5^2 + 0.707^2} = 0.9999$ , which is close to unity as expected since the absolute values of all the elements in a given column are same (del Toro Iniesta 2003). The values of matrix elements  $\mathbf{O}^\pm$  are not the same at different wavelengths and hence the maximum efficiencies of modulation scheme in measuring Stokes QUV are different. However, the total polarimetric efficiency will remain close to unity.

For comparison, the maximum efficiencies of some of the well known polarimeters are given below: ASP-(1.0, 0.546, 0.41, 0.659), ZIMPOL-(1.0, 0.474, 0.467, 0.534), TIP-(1.0, 0.617, 0.41, 0.659), POLIS-(1.0, 0.494, 0.464, 0.496). In the above examples, only TIP has a total polarimetric efficiency close to unity.

## 2.2 Demodulation

The demodulation of the input Stokes parameters from the modulated intensities involve the following steps. As a first step, the signal vectors  $\vec{S}^\pm$  (Gandorfer 1999; Stenflo 1984) of the orthogonally polarised beams are constructed from the modulated intensities (Eq. 1) using the equation,

$$\vec{S}^\pm = \mathbf{D}\vec{I}^\pm/8 \quad (2)$$

where the matrix  $\mathbf{D}$  is defined as,

$$\mathbf{D} = \begin{pmatrix} 1.0 & 1.0 & 1.0 & 1.0 & 1.0 & 1.0 & 1.0 & 1.0 \\ 1.0 & -1.0 & -1.0 & 1.0 & 1.0 & -1.0 & -1.0 & 1.0 \\ -1.0 & 1.0 & -1.0 & 1.0 & -1.0 & 1.0 & -1.0 & 1.0 \\ 1.0 & -1.0 & -1.0 & 1.0 & -1.0 & 1.0 & 1.0 & -1.0 \end{pmatrix}.$$

One can see from the matrix  $\mathbf{D}$  that, to derive signal vectors all the eight stage intensity measurements are considered. Hence the final derived input Stokes parameters will be well balanced with respect to changes, if there are any, during measurements in the input Stokes parameters. Also, the final derived Stokes parameters will be an average over the time taken for the eight stages of modulation.

The second step involves combining the signal vectors of the orthogonally polarized beams after correcting for the gain factors  $g^\pm$ . Gain table corrections can be done either by regular flat field procedure or normalizing the elements of signal vectors to their respective first element (i.e.  $\vec{S}^\pm/S^\pm(0)$ ). Since the regular flat field procedure limits the polarimetric precision and to make use of the advantage of the beam swapping technique incorporated in the modulation scheme, second method is used to derive the combined signal vector. The signal vector ( $\vec{S}'$ ) of the combined beam can be written as

$$\begin{aligned} S'(0) &= S^+(0) + S^-(0) \\ S'(1) &= S^+(1)/S^+(0) - S^-(1)/S^-(0) \\ S'(2) &= S^+(2)/S^+(0) - S^-(2)/S^-(0) \\ S'(3) &= S^+(3)/S^+(0) - S^-(3)/S^-(0) \end{aligned} \quad (3)$$

where  $S'(i)$ ,  $i = 0, 1, 2, 3$ , are the elements of  $\vec{S}'$ . Similarly  $S^\pm(i)$  are defined. The indices  $i = 0, 1, 2, 3$  are correspond to the Stokes parameters I, Q, U, V respectively.

However, the flat field corrections are essential for the total intensity. With the definitions of Eq.(3), the signal vector of the combined beam can be written in terms of the input Stokes vector as (Gandorfer, 1999 and Stenflo, 1984),

$$\vec{S}' = \mathbf{M}\vec{S}'_{in} \quad (4)$$

where  $\vec{S}'_{in} = [I, Q/I, U/I, V/I]^T$  is the input Stokes vector and  $\mathbf{M}$  is a  $4 \times 4$  matrix known as the response matrix of the polarimeter. The theoretical response matrix at the design wavelength is given by

$$\mathbf{M} = \begin{pmatrix} 1 & 0 & 0 & 0 \\ 0 & 0.5 & 0 & 0 \\ 0 & 0 & 0.5 & 0 \\ 0 & 0 & 0 & 0.707 \end{pmatrix}.$$

The third and final step involves obtaining the input Stokes vector( $\vec{S}'_{in}$ ) from Eq.(4). During the observations, the response matrix is obtained using a polarimetric calibration procedure which will be detailed in Section 4.

### 2.3 Polarimetric efficiency

The efficiency of the polarimeter in measuring respective Stokes parameter is defined as (Beck et al. 2005)

$$\epsilon_i = \sqrt{\sum_{j=1,4} \mathbf{M}_{ji}^2} \quad (5)$$

where  $i = 0, 1, 2, 3$  corresponds to I, Q, U, V respectively. Since the response matrix  $\mathbf{M}$  in Eq.(4) is diagonal, the efficiency in the Eq. (5) will be simplified (using Eq. 4) to

$$\epsilon_i = |S'(i)/S'_{in}(i)|. \quad (6)$$

We would like to note here that the response matrix  $\mathbf{M}$  in Eq.(4) is diagonal at all the wavelengths considered here. However, at the wavelengths away from the design wavelength, the signals  $S^\pm(0)$  in Eq.(2) are not just proportional to input Stokes I but with a small contribution from the input Stokes Q. If the signal vectors( $\vec{S}^\pm$ ) of orthogonally polarised beams are combined without normalising to their respective Stokes I signal then this cross-talk term will not appear in the signal vector( $\vec{S}'$ ) of the combined beam. But, the flat fielding is essential to remove the gain factors  $g^\pm$ . In this paper the signal vectors are combined in such a way that the Stokes QUV signals are normalised to Stokes I signal in order to remove the gain factors. This results in an over estimation of efficiency  $\epsilon_Q$ . This over estimation is about 1.8% at  $\lambda 4500$ , 0.15% at  $\lambda 5000$ , 0.65% at  $\lambda 5500$ , 0.24% at  $\lambda 5890$ , 0.1% at  $\lambda 6563$  and 0.6% at  $\lambda 7000$ . These wavelengths are chosen because, the efficiencies are measured at these wavelengths through the experiment presented in the next section. In the regular solar observations the Stokes Q signal is smaller than Stokes I at least by an order of magnitude, the cross-talk from Q to I will be often negligible.

## 3. Laboratory experiment

The efficiency of the polarimeter is different for different wavelengths due to the chromatic nature of the retarders used in the polarimeter. If the polarimeter is used at different wavelengths then it is important to understand its performance at the desired wavelength. The variation of the efficiency factor for different input Stokes parameters is studied by carrying out a few laboratory experiments.

The experimental setup is shown in Fig.1. The light from the monochromator was set at the desired wavelength and then passed through a 1 mm rectangular aperture. This rectangular aperture was imaged on to a CCD detector using a two lens system

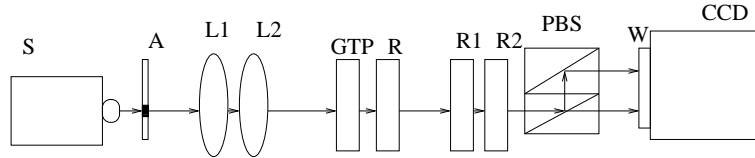


**Figure 1.** Block diagram of an experimental setup used to study the polarimetric efficiency. The symbols in the figure are S-monochromator, A-mount holding a 1 mm square aperture, L1 and L2-lenses ( $f=25\text{cm}$ ), GTP-Glan Thomson prism used to produce linear polarization, R-QWP used along with GTP to produce circular polarization, R1 and R2- Half and Quarter waveplates which forms a part of the polarimeter, PBS-polarizing beam splitter, W- CCD window.

with an effective focal length of 12.5 cm. The polarimeter optics were placed between the lens and the detector. The first in the light beam is the QWP (R1), followed by the HWP (R2) and the PBS. The retarders (R1 and R2) of the polarimeter were mounted on two different rotating stages whose rotational accuracy is  $0.1^\circ$ . A known state of polarization was produced using the GTP and calibration retarder (CU) R. Stokes  $Q$  and  $U$  were produced by using only the GTP whereas both GTP and R were used to produce Stokes  $V$ . (The CU retarder is a zero order chromatic waveplate which acts as a quarter waveplate at  $\lambda 6300$ . This is the same quarter waveplate which was earlier used in the single beam polarimeter installed at Kodaikanal by Sankarasubramanian(2000) and the characteristics of the waveplate is presented there. The retardance of the CU retarder at other wavelengths is calculated by the well known linear relation, see for eg. in Hetch 2002). Eight measurements, for each input Stokes parameter, were performed by positioning the retarders (R1 and R2) at different angles as shown in Table 1.

The measured data were first corrected for dark current. Then the Stokes signal vectors correspond to the orthogonally polarised beams were obtained from the measured intensities and the matrix  $\mathbf{D}$  using Eq.(2). The corresponding Stokes QUV signals were normalised to the respective Stokes I signal as in Eq.(3).

We noted in section 2.3 that the theoretical response matrix of the polarimeter presented in this paper is diagonal at all the wavelengths considered. However, in practice there will be off-diagonal elements which are nothing but the cross-talk among Stokes parameters. But, in the experiment performed to study the polarimetric efficiency, the measured cross-talk terms are small. Since the cross-talk terms are small, the simplified definition of Eq.(6) is used to calculate the efficiency.

Plots of polarimetric efficiency in measuring Stokes  $Q$ ,  $U$  and  $V$  as a function of wavelength are shown in Fig.2. The diamond symbols shown in the plots are the experimental values and the solid lines are theoretical curves. It is clear from the plot that the experimental values closely resemble the theoretical predictions. From this figure it can be concluded that  $Q$  and  $V$  are measured with better efficiencies in longer wavelength region compared to the design wavelength, whereas  $U$  is measured better at shorter wavelengths.

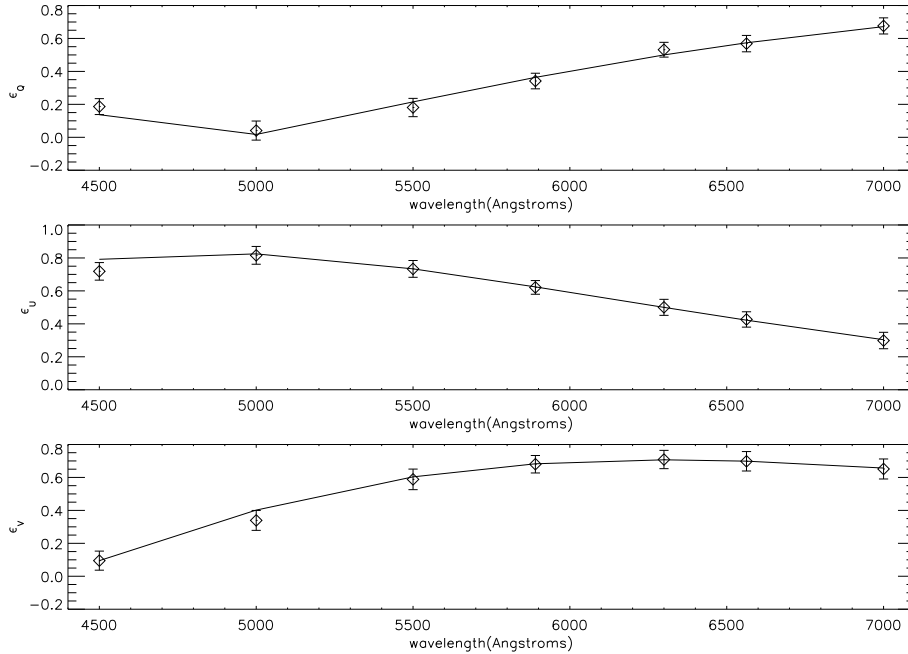


**Figure 2.** Plots of polarimetric efficiency of Stokes  $Q$ ,  $U$  and  $V$  parameters as a function of wavelength. The solid curves are theoretical values whereas the diamond symbols correspond to the measured values. The error bars shown in these plots are ten times the obtained noise rms values.

#### 4. Calibration of the polarimeter installed at KTT

The calibration of the polarimeter, which uses the modulation scheme presented in section 2, installed as a backend instrument at KTT is discussed in this section. KTT is a three mirror coelostat system for solar observations (Bappu 1967). It is equipped with a Littrow mount spectrograph using a grating of 600 lines per mm. The polarimeter setup is placed in the converging beam ( $f/90$ ) of the telescope before the spectrograph slit. The retarders are mounted on rotating stages which can be rotated from  $0$  to  $360^\circ$  in steps of  $22.5^\circ$ . PBS is fixed in position with one of its optic axes parallel to the slit direction. A linear polarizer, called as a compensator, is placed behind the PBS to compensate for the differential grating efficiency of the two orthogonally polarized beams. The compensator is oriented at  $45^\circ$  to the grating grooves to make the efficiency of the orthogonal beams nearly equal. Ideally a QWP or a HWP will be preferred as the compensator. But, linear polarizer is used to make use of the polarimeter at other wavelengths of interest.

To calibrate the polarimeter, a calibration unit consisting of a linear polarizer followed by a quarter waveplate at  $\lambda 6300$ , was used. The optical axis of the linear polarizer was

aligned with one of the optic axes of the PBS. Keeping the polarizer at this orientation, the linear retarder was rotated from  $0^\circ$  to  $180^\circ$  in steps of  $15^\circ$  and hence producing 13 input states of polarisation. Out of 13 states of polarisation, only 11 are different because the polarisation states correspond to the retarder orientation  $0^\circ$ ,  $90^\circ$  and  $180^\circ$  are essentially the same. The corresponding input Stokes parameters and measured Stokes signals (Eq. 3) are arranged in a  $13 \times 4$  matrix form and solved for response matrix of the polarimeter as follows(Beck et al. 2005). If  $\mathbf{S}_{in}^c$  represents the  $13 \times 4$  input Stokes matrix and  $\mathbf{S}_{op}^c$  represents the measured  $13 \times 4$  signal matrix then,

$$\mathbf{S}_{op}^c = \mathbf{S}_{in}^c \mathbf{M}^T. \quad (7)$$

The response matrix of the polarimeter setup ( $\mathbf{M}$ ) is solved by defining  $(\mathbf{S}_{in}^c)^T \mathbf{S}_{op}^c = (\mathbf{S}_{in}^c)^T \mathbf{S}_{in}^c \mathbf{M}^T = \mathbf{S} \mathbf{M}^T$  as (see Beck et al. 2005 for details)

$$\mathbf{M}^T = \mathbf{S}^{-1} (\mathbf{S}_{in}^c)^T \mathbf{S}_{op}^c \quad (8)$$

where,  $\mathbf{S} = (\mathbf{S}_{in}^c)^T \mathbf{S}_{in}^c$ . The structures of  $\mathbf{S}_{in}^c$  and  $\mathbf{S}_{op}^c$  are given in the appendix for the sake of clarity.

#### 4.1 Measurement of response matrix of the polarimeter

The calibration data were obtained using the procedure as explained in the beginning of this section. Data was subjected to the standard dark and flat corrections(for eg. see Beck et al. 2005). The response matrix of the polarimeter setup has been derived using the  $13 \times 4$  input Stokes matrix( $\mathbf{S}_{in}^c$ ) constructed out of input Stokes parameters and  $13 \times 4$  signal matrix( $\mathbf{S}_{op}^c$ ) constructed out of measured Stokes signals using Eq.(8). A typical derived response matrix( $\mathbf{M}$ ) of the polarimeter setup is,

$$\begin{pmatrix} 1 & -0.0066 & 0.0384 & 0.0461 \\ 0.0048 & 0.5643 & 0.0565 & -0.0016 \\ 0.0074 & -0.0084 & 0.4173 & -0.0065 \\ -0.0053 & -0.0037 & 0.0248 & 0.6835 \end{pmatrix}.$$

The wavelength of observation is in the continuum of  $\lambda 6563$  wavelength region. The fit error of the second, third and fourth column of the response matrix, which are nothing but the errors in the determination of Stokes  $QUV$ , are 0.0044, 0.0048 and 0.0022 respectively. The corresponding noise rms of the measurements are 0.0017, 0.0018 and 0.0023 respectively.

The observed efficiency(Eq.5) of the polarimeter in measuring Stokes  $QUV$  are 0.5644,

0.4228 and 0.685086 respectively, which are close to theoretically expected values of 0.573, 0.423 and 0.698 at this wavelength. In an ideal case, off-diagonal elements of the response matrix  $\mathbf{M}$  are expected to be zero. However, in practice telescope induced cross-talk and the variation in the sky transparency can influence the calibration of the polarimeter. Sky transparency variation means that the variation in the input intensity to the telescope. To take into account the telescope induced cross-talk, telescope model of KTT originally developed by Balasubramaniam et al.(1985) and later modified by Sankarasubramanian(2000) is used. A computer simulation has been performed to understand the effect of sky transparency variation on the calibration of the polarimeter. From this simulation it is found that the maximum cross-talk produced among Stokes parameters is  $\approx 1.8\%$  for a sky transparency variation of 14% within the eight stages of measurement. In the actual measurements for this calibration, the intensity variation is of the order of 14%. The origin of most of the off-diagonal elements  $\mathbf{M}$ , can be explained based on the sky transparency variation. However, there are off-diagonal elements which are larger than the 1.8% expected due to the sky transparency variation. An off set angle of  $\approx -1.5^\circ$  in the HWP is required to produce the observed cross-talk from  $U$  to  $Q$ . However, the origin of cross-talk from  $U$  to  $V$  has not been traced out.

## 5. Conclusions

An eight stage modulation scheme to measure the general state of polarization is presented here. Beam swapping technique is incorporated in this scheme, which helps in alleviating the gain correction errors. The total polarimetric efficiency is close to unity as the Stokes parameters are weighted equally in all the stages of modulation. The final Stokes parameters are demodulated using all the stages of intensity measurements. Hence, the derived input Stokes parameters are equally weighted time averaged quantities over the time of measurement.

Since the retarders used in the polarimeter are chromatic, the efficiency of the polarimeter in measuring Stokes  $QUV$  is wavelength dependent. The laboratory experiments performed to study the wavelength dependence of efficiency of the polarimeter confirms the theoretical expectations.

It is found through computer simulation that a 14% sky transparency variation can cause  $\approx 1.8\%$  uncertainty in the elements of the polarimetric response matrix during its calibration, for the modulation/demodulation scheme presented here. The non-zero values of the off-diagonal elements are not a serious concern if those values do not change drastically in short time scales. During any solar polarimetric measurements, data for the calibration of the polarimeter are taken at least once a day. Calibration of the polarimeter are carried out on a few days over a period of 10-day and the response matrix derived over this period did not show any appreciable variations. The variations in the off-diagonal elements are less than the fit errors ( $< 0.5\%$ ). The polarization signals observed on the

Sun is always less than 40% and hence an uncertainty of 0.5% in the calibration will produce an inaccuracy of 0.2% in the polarization signals.

The measured total polarimetric efficiency of the polarimeter installed at KTT is  $\approx 0.986$  at  $\lambda 6563$  wavelength region which is better than some of the polarimeters such as ZIMPOL(0.72), ASP(0.88), TIP(0.92) and POLIS(0.84).

### Acknowledgments

We would like to thank the anonymous referee for the useful suggestions which made the contents of the paper clearer. We thank B. R. Prasad and Ravinder Kumar Baynal for providing some of the laboratory equipments necessary for the experiment and P. K. Mahesh for his help in procuring the laboratory equipments. We thank P. U. Kamath for his help in mechanical design and fabrication of the polarimeter. The help of P. Devendran and P. Hariharan during observations are thankfully acknowledged.

### References

- Balasubramaniam, K. S., Venkatakrisnan, P & Bhattacharya, J. C., 1985, *SoPh*, 99, 333  
 Bappu, M. K. V., 1967, *SoPh*, 1, 151  
 Beck, C., Schmidt, W., Kentischer, T. & Elmore, D. F., 2005, *A&A*, 437, 1159  
 Bianda, M., Solanki, S. K. & Stenflo, J. O., 1998, *A&A*, 331, 760  
 Bruce W., & Lites, 1987, *ApOpt*, 26, 3838  
 Donati, J. F., Semel, M., Rees, D. E., Taylor, K & Robinson, R. D., 1990, *A&A*, 232, L1  
 Elmore, D. F., Bruce W. Lites, Tomczyk, S., Skumanich, A. P., Dunn, R. B., Schuenke, J. A., Streander, K. V., Leach, T. W., Chambellan, C. W., Hull, H. K. & Lacey, L. B., 1992, in *Polarization analysis and measurement*, eds G. H. Goldstein, & R. A. Chipman, SPIE, 1746, 22  
 Gandorfer, A. M., 1999, *Opt. Eng.*, 38, 1402  
 Hetch, E., 2002, in *Optics*, chapter 8, Pearson education Asia publisher  
 Martinez Pillett, Collados, M., Sanchez Almeida, J., Gonzalez, V., Chuz-Lopez, A., Manescau, A., Joven, E., Paez, E., Diaz, J. J., Feeney, O., & Sanchez, V., 1999, in *High resolution solar physics: Theory, observations and techniques*, eds T. R. Rimmele, et al., ASP conference series, 183, 264  
 del Toro Iniesta, J. C. & Collados, M., 2000, *Applied Optics*, 39, 1637  
 del Toro Iniesta, J. C., 2003, *Introduction to spectropolarimetry*, Cambridge university press  
 Sankarasubramanian, K., 2000, Phd thesis, Bangalore university, India  
 Sankarasubramanian, K., Elmore, D. F., Lites, B. W., Sigwarth, M. Rimmele, T., Hegwer, S., Gregory, S., Streander, K. V., Wilkins, L. M., Richards, K., & Berst, C., 2003, in *Polarimetry in Astronomy*, Eds Silvano Fineschi, SPIE 4843, 414  
 Semel, M., Donati, J. F., & Rees, D. E., 1993, *A&A*, 278, 231  
 Stenflo, J. O., 1994, *Solar magnetic fields: Polarised radiation diagnostics*, Kluwer  
 Stenflo, J. O. & Povel, H., 1985, *ApOpt*, 24, 3893  
 Stenflo, J. O., 1984, *ApOpt*, 23, 1267

### Appendix

The structure of the measured Stokes signal matrix in Eq. (7) is given by

$$\mathbf{S}_{op}^c = \begin{pmatrix} S_{op}^1(0) & S_{op}^1(1) & S_{op}^1(2) & S_{op}^1(3) \\ S_{op}^2(0) & S_{op}^2(1) & S_{op}^2(2) & S_{op}^2(3) \\ S_{op}^3(0) & S_{op}^3(1) & S_{op}^3(2) & S_{op}^3(3) \\ S_{op}^4(0) & S_{op}^4(1) & S_{op}^4(2) & S_{op}^4(3) \\ S_{op}^5(0) & S_{op}^5(1) & S_{op}^5(2) & S_{op}^5(3) \\ S_{op}^6(0) & S_{op}^6(1) & S_{op}^6(2) & S_{op}^6(3) \\ S_{op}^7(0) & S_{op}^7(1) & S_{op}^7(2) & S_{op}^7(3) \\ S_{op}^8(0) & S_{op}^8(1) & S_{op}^8(2) & S_{op}^8(3) \\ S_{op}^9(0) & S_{op}^9(1) & S_{op}^9(2) & S_{op}^9(3) \\ S_{op}^{10}(0) & S_{op}^{10}(1) & S_{op}^{10}(2) & S_{op}^{10}(3) \\ S_{op}^{11}(0) & S_{op}^{11}(1) & S_{op}^{11}(2) & S_{op}^{11}(3) \\ S_{op}^{12}(0) & S_{op}^{12}(1) & S_{op}^{12}(2) & S_{op}^{12}(3) \\ S_{op}^{13}(0) & S_{op}^{13}(1) & S_{op}^{13}(2) & S_{op}^{13}(3) \end{pmatrix}.$$

And that of input Stokes matrix is given by

$$\mathbf{S}_{in}^c = \begin{pmatrix} S_{in}^1(0) & S_{in}^1(1) & S_{in}^1(2) & S_{in}^1(3) \\ S_{in}^2(0) & S_{in}^2(1) & S_{in}^2(2) & S_{in}^2(3) \\ S_{in}^3(0) & S_{in}^3(1) & S_{in}^3(2) & S_{in}^3(3) \\ S_{in}^4(0) & S_{in}^4(1) & S_{in}^4(2) & S_{in}^4(3) \\ S_{in}^5(0) & S_{in}^5(1) & S_{in}^5(2) & S_{in}^5(3) \\ S_{in}^6(0) & S_{in}^6(1) & S_{in}^6(2) & S_{in}^6(3) \\ S_{in}^7(0) & S_{in}^7(1) & S_{in}^7(2) & S_{in}^7(3) \\ S_{in}^8(0) & S_{in}^8(1) & S_{in}^8(2) & S_{in}^8(3) \\ S_{in}^9(0) & S_{in}^9(1) & S_{in}^9(2) & S_{in}^9(3) \\ S_{in}^{10}(0) & S_{in}^{10}(1) & S_{in}^{10}(2) & S_{in}^{10}(3) \\ S_{in}^{11}(0) & S_{in}^{11}(1) & S_{in}^{11}(2) & S_{in}^{11}(3) \\ S_{in}^{12}(0) & S_{in}^{12}(1) & S_{in}^{12}(2) & S_{in}^{12}(3) \\ S_{in}^{13}(0) & S_{in}^{13}(1) & S_{in}^{13}(2) & S_{in}^{13}(3) \end{pmatrix}.$$

where  $S_{op}^j(i)$  and  $S_{in}^j(i)$ ,  $j = 1, \dots, 13$  correspond to 13 orientations of the calibration retarder and  $i = 0, 1, 2, 3$  corresponds to Stokes I, Q, U, V are the measured Stokes signals and input Stokes parameters respectively.